Chemical Physics Letters 684 (2017) 304–309

Contents lists available at ScienceDirect

Chemical Physics Letters

journal homepage: www.elsevier.com/locate/cplett

Research paper

A structural and theoretical study of the alkylammonium nitrates forefather: Liquid methylammonium nitrate

Lorenzo Gontrani [a,*], Ruggero Caminiti [a,b], Umme Salma [a], Marco Campetella [a,c]

[a] Università degli Studi di Roma "La Sapienza", P. le Aldo Moro 5, I-00185 Roma, Italy
[b] Centro di Ricerca per le Nanotecnologie Applicate all'Ingegneria CNIS, Università di Roma "La Sapienza", P. le Aldo Moro 5, I-00185 Roma, Italy
[c] Chimie ParisTech, PSL Research University, CNRS, Institut de Recherche de Chimie Paris, F-75005 Paris, France

ARTICLE INFO

Article history:
Received 22 May 2017
In final form 5 July 2017
Available online 6 July 2017

Keywords:
X-ray
Nitrate
Methylammonium
Melted
AIMD

ABSTRACT

We present here a structural and vibrational analysis of melted methylammonium nitrate, the simplest compound of the family of alkylammonium nitrates. The static and dynamical features calculated were endorsed by comparing the experimental X-ray data with the theoretical ones. A reliable description cannot be obtained with classical molecular dynamics owing to polarization effects. Contrariwise, the structure factor and the vibrational frequencies obtained from *ab initio* molecular dynamics trajectories are in very good agreement with the experiment. A careful analysis has provided additional information on the complex hydrogen bonding network that exists in this liquid.

1. Introduction

The latvian/russian/german chemist Paul Walden is generally recognized as one of the "fathers" of that class of (organic) molten salts that most contemporary chemists would call "ionic liquids". As a matter of fact, Walden, in his 1914 seminal work [1] described a series of water-free salts with a melting point below 100 °C, and only one of such compounds can be considered as RTIL ("Room Temperature Ionic Liquid") in the modern sense, namely the widely renowned ethylammonium nitrate (EAN). A period of at least thirty years passed before new ionic liquids were discovered, but in the following few decades a large body of scientific literature on these compounds flourished, given the large range of varied and peculiar properties they posess [2–10].

In this study we focus on one of the molten salts described by Walden (on page 416), methylammonium nitrate (CH_3NO_3, termed as MAN or MMAN in the subsequent literature, see Fig. 1). This system is the one-carbon representative of the family of monoalkylammonium nitrates, that includes three room-temperature liquids, ethylammonium nitrate (EAN, object of Walden studies itself), propylammonium nitrate (PAN) and butylammonium nitrate (BAN), and belongs to the subgroup of protic ionic liquids (PILs) [11–14]. All these systems are obtained from the proton transfer reaction between the *Brønsted acid* nitric acid and the *Brønsted base* alkylamine. MAN is instead solid at room temperature, but it undergoes a solid I solid II phase transition at 352 K, turning into a "ionic plastic phase" which shows very large mobility, as assessed by two NMR studies [15,16]. The melting temperature reported by Walden in his work (80 °C) is probably ascribable to this phase transition. Finally, around 384 K (natural sample, [17] rechecked by us) or 391 K (ND_3 deuterated sample [15]) the isotropic liquid is obtained. A limited number of papers on liquid MAN are found in the literature, among which we cite an *ab initio* molecular dynamics (AIMD) study [18], a Raman coupled to powder diffraction study interpreted with *ab initio* calculations [19], while no liquid diffractions measurements have yet been reported. To fill this gap, we report in this article, for the first time, the experimental X-ray diffraction pattern of liquid MAN. Though it should not be regarded as an ionic *liquid* as said before, the knowledge of the liquid phase structure of this prototypical compound is of utmost interest, and was also selected as a benchmark to test the capabilities of our new high-speed EDXD diffractometer. This choice was made also considering that the smaller dimension of the system, with respect to longer chain alkylammonium nitrates, allows more thorough computational studies capable of interperting the X-ray patterns more accurately.

Indeed, a general problem we encounter when studying ILs, particularly those capable of giving H-bond interactions, with computational techniques is represented by the fact that it is rather difficult to obtain reliable results using the current pairwise

* Corresponding author.
E-mail addresses: lorenzo.gontrani@uniroma1.it (L. Gontrani), marco.campetella@uniroma1.it (M. Campetella).

http://dx.doi.org/10.1016/j.cplett.2017.07.017
0009-2614/

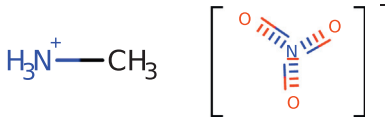

Fig. 1. Sketch of cation and anion.

potentials. Such kind of approach, actually, cannot reproduce in an appropriate way polarization and many body effects [18,20–22], and often further modifications are required, like using three-body terms for H-bonds [23] or polarizable potentials [13], though some successful calculations on longer alkylammonium nitrates have been reported [24].

Therefore, considering the problems with ordinary force field treatment and the after all affordable dimension of the system, we decided to perform an AIMD simulation, obtaining in this way a detailed description of the liquid bulk phase and of the underlying interactions, particularly with regard to the hydrogen bond network established between cation and anion, and providing the infrared spectra of the liquid through the vibrational density of states (VDOS), calculated by Fourier transforming the velocity autocorrelation functions.

1.1. Experimental details

The X-ray experiments were performed on a new Energy-Dispersive diffractometer recently set up in our lab at Rome "La Sapienza" university. The instrument has a novel horizontal design that permits data acquisitions at the three to four fixed angular configurations needed by the technique [25,26] in parallel, very rapidly and at large momentum transfer range, namely between 0.15 and 24 $Å^{-1}$ (see Fig. 2).

The open configuration of the instrument allows the easy use of additional equipment, such as the spot fan heater used to melt and keep the sample liquid. The magnitude of the transferred momentum, Q, depends on the scattering angle according to the relation $Q = 4\pi sin(\theta)/\lambda$, approximately equal to ≈1.0136 E sin θ, when E is expressed in keV and Q in $Å^{-1}$. The marked increase of the intensity of this new instrumental configuration allows to collect a complete diffraction pattern at high statistics (*viz* more than 500,000 counts), in at most 6 h. The sample was put in a quartz capillary, and the beam was focussed on the liquid portion at the center of the capillary, surrounded by solid phases above and below. After the data treatment, the structure function I(Q) was obtained, which is sensitive to the pairwise distances between the atoms of the system:

$$I(Q) = \sum_{i=1}^{N}\sum_{j=1}^{N} x_i x_j f_i f_j \times \left[4\pi\rho_0 \int_0^\infty r^2 (g_{ij}(r) - 1)\frac{sinQr}{Qr} dr\right] \quad (1)$$

The radial distribution profile, in differential form, was obtained by I(Q) Fourier Transform:

$$Diff(r) = \frac{2r}{\pi}\int_0^\infty QI(Q)M(Q)rsinQdQ \quad (2)$$

In the formulae above, x_i are the numerical concentrations of the species, f_i their Q-dependent X-ray scattering factors and ρ_0 is the bulk number density of the system. To improve the curve resolution at high Q, and to decrease the truncation errors, both the experimental and the theoretical structure functions were multiplied by a sharpening function $M(Q) = \frac{f_N^2(0)}{f_N^2(Q)} exp(-0.01Q^2)$.

This methodology has been successfully applied to the study of molecular [27] and ionic liquids [28], as well as solutions [29].

1.2. Computational details

In this work, a computational protocol analogous to what was used for previous articles was exploited [9,30], that will be briefly summarized here. Two types of molecular dynamics (MD) simulations were performed, as already pointed out in the Introduction. In the first step, a classical molecular dynamics was carried out on a box composed of 32 ILs with AMBER and the Gaff force field [31]. Though the charge distribution is particularly important in classical MD simulation of highly charged systems as ILs [28], for this small cation only the single staggered conformation (absolute minimum) was used to derive the point charges using the RESP procedure. The starting simulation cell was built with the PACKMOL software [32] and was then equilibrated for 5 ns in an isothermic-isobaric ensemble (NPT) at 385 K. Finally a productive trajectory of 2 ns in the canonical ensemble (NVT) was produced. The final theoretical density was 1.42 g/cm^3, corresponding to a box edge around 15.2 Å, and differed from the value we estimated at the same temperature by weighing a known volume of the liquid (1.38) by about 3%. Indeed, even though the final aim of our study was an *ab initio* simulation as described above, a "preparatory" study with classical MD is almost always needed to equilibrate the simulation boxes. The final configuration of the classical trajectory was used as the starting point for the *ab initio* simulations, that were performed with CP2k [33], using the Quickstep module and the orbital transformation [34]. PBE density functional was used for the electronic calculation, with the empirical dispersion correction (D3) by Grimme [35]. MOLOPT-DZVP-SR-GTH basis sets and GTH pseudopotentials [36] were applied; a 0.5 fs time step

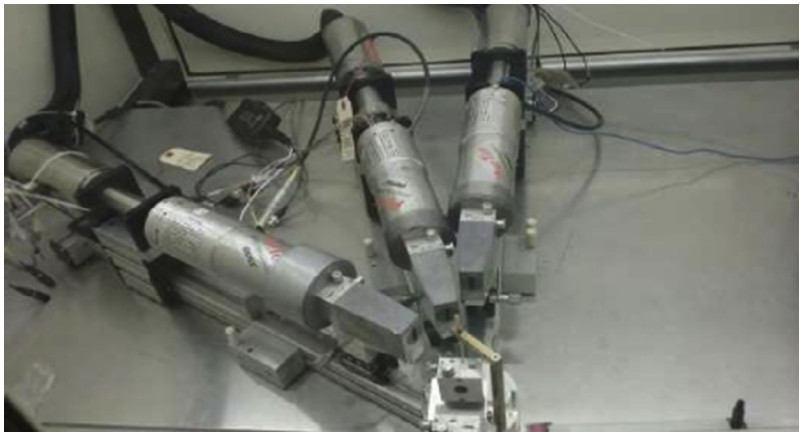

Fig. 2. The new EDXD diffractometer with three simultaneous detectors.

was employed, and the simulation temperature was held constant by a Nosé-Hoover chain thermostat. The *ab initio* simulations were performed at 450 K, around 60 degrees above the melting point, to accelerate the dynamics of the viscous liquid (as in [18]). An equilibration of 7 ps was performed at first, followed by a 60 ps productive simulation. This protocol was already adopted and validated by comparison with X-ray data in previous works [9,21,30]. Clearly, in such rather short simulation time (though not at all trivial for AIMD) the phase space exploration is limited and the configurations depend on the previous classical calculation. Though, AIMD improves the description of the short-medium range structural correlations when electronic effects play a role. The vibrational spectra of the ions was calculated with the MOLSIM package [37], by projecting the VDOS onto the molecules effective normal modes [30] with the MOLSIM package [37]. For more details read Ref. [30].

2. Results

In Fig. 3 we report both the experimental and the theoretical function described in Experimental Details. The structure factor, QI(Q)M(Q), is shown on top, while the radial distribution function Diff(r), is on bottom. The experimental data is represented in black, and the two models are in green (classical MD) and in red (AIMD).

The first evident feature in Fig. 3, is the very satisfactory reproduction of the experimental data, both QI(Q)M(Q) and Diff(r), by the *ab initio* model. Conversely, classical MD cannot reproduce either patterns. This failure is probably attributable to the inherent nature of the MAN, whose organic moiety is composed of the methyl group only, so that classical force fields, generally developed for organic molecules, fail in describing the structural parameters. In particular, the accuracy is poorer in the central range between 3 Å and 5 Å, where an almost featureless peak is obtained. This issue was already discussed in a former X-ray/classical MD study on EAN [23], where the incomplete description of the hydrogen bond interaction between ammonium and nitrate was improved adding a three-body term to the potential. To investigate the effect of model size, we performed a control simulation with the same force field using a larger box (edge around 38 Å), containing 400 ion pairs. The patterns obtained for this enlarged model show only a slight improvement in the central range (3–5 Å), namely the featureless peak turns into two small shoulders, but still the directionality of H-bonds [23] is not accounted for satisfactorily. Furthermore, the large model overemphasizes the long-range interactions, resulting in a too structured system, as pointed out by the very strong periodicity in the Diff(r) pattern. Most probably, the increase of box dimensions can reduce the finite size periodicity artifacts of short range interactions only, while it may not be sufficiently large for long range interactions, that can experience large artifacts in highly charged systems [38]. The labels "small box" and "large box" in Fig. 3 refer to these two models.

If we analyze the curves in more detail, we can point out the following characteristics: (1) presence of the principal peak (often called "Adjacency" peak, as in [39]) at 1.80 $Å^{-1}$ and absence of "pre-peaks" before, both in experiment and model, and (2) the presence of two smaller peaks (2.67 and 4.24 $Å^{-1}$), in both data as well. For the first time we have shown the effective absence of a medium-long range order for alkylammonium nitrate IL, with alkyl chain shorter than ethyl group. Such phenomenom was just predicted in previous theoretical articles [18], but we have now the direct proof from experimental data. The second feature can be related to space correlations ranging from 3 Å to 5 Å. For protic ionic liquids, cation-anion hydrogen-bond interactions can give rise to those peaks [23]. Regarding the experimental radial pattern (Fig. 3, bottom), we can point out a short-ranged shell structure for this liquid, with correlation fading off after 9 Å; for this reason, the smaller box, of edge of about 15.2 Å, to which corresponds a correlation distance of 7.6 Å according to Periodic Boundary Conditions formalism, was considered appropriate for the AIMD simulation, as it was computationally affordable though capable of covering most of the correlation. The second feature of I(Q) gives rise to the two quite evident shoulders located at 3.40 and 4.73 Å respectively, owing to the contacts among the hetero atoms of ammonium

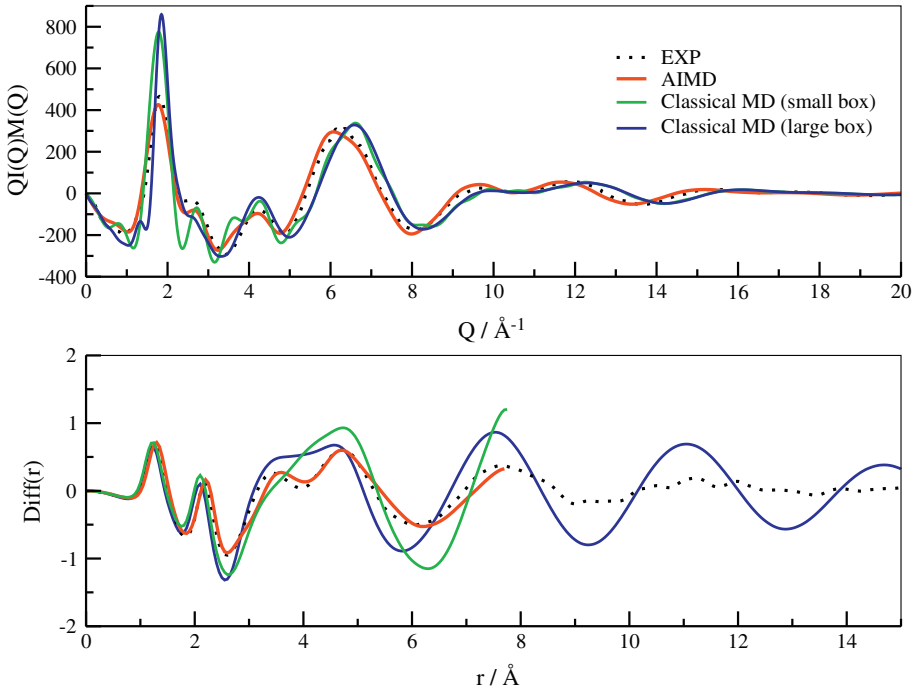

Fig. 3. Top panel: Structure function. Bottom panel: Radial distribution function.

and nitrate group. After its validation with X-ray data, at least in the first two coordination shells, we could use the AIMD model to gather some structural information. The simplest geometric information available is the radial distribution functions (RDF).

Three different radial distribution functions are represented in Fig. 4: the first shows the correlation between the hetero atoms of cation and anion, the second one describes the distance between the nitrogen atoms of anions, while the last RDF represents the correlation between the carbon atoms of the cations. The *ab initio* simulation shows a well-defined first coordination shell of nitrate anions surrounding the ammonium group. The equilibrium distance is about 2.8 Å, and it is in agreement with some of the previous data from literature [30,40]. As shown in previous works [13], such interaction can be classified as a strong hydrogen bond. Turning to the other two RDFs, we can see a completely different behavior: the anions exhibit a faint and broad peak located at about 5.3 Å, while the aliphatic moieties do not show a neat spatial correlation (absence of peaks). To summarize, in such system the ammonium-nitrate interaction is the most important one. The other kinds of aggregation are very weak or absent. This finding complies with the failure of the classical modeling of the structure factor: in MAN it is necessary to resort to *ab initio* molecular dynamics to describe the leading interaction occurring between the two rather "short" charged groups that are hard to model with the classical two-body potential. To provide a more quantitative description of the interaction we have calculated the following quantities:

- The number of oxygen atoms coordinated to the ammonium nitrogen atom, by integrating the first peak of $N—H_3^+\cdots O$ RDF, which is 3.02.
- The number of H-bond-like contacts within a given ion pair, averaged along the trajectory, (1.9). The structural parameters (distance and angle cutoffs) chosen to characterize the H-bond contacts are: the N···O distance, with an upper limit of 3.5 Å and the N—H···O angle, ranging from 135° to 180°. Such analysis was carried out with the VMD package [41].
- The hydrogen-bond lifetime. For this purpose, we used TRAVIS autocorrelation function tool [42]. The relative autocorrelation function was fitted with the following function: $C(t) = Ae^{(-\frac{t}{\tau 1})} + (1-A)e^{(-\frac{t}{\tau 2})}$, where t is time, A is a constant that determines the occurrence probability of the process, $\tau 1$ and $\tau 2$ are the time constants of the two processes. Process 1 ($\tau 1$), which is fast, represents the hydrogen bond breaking, while the slower process 2 is the migration of the ionic pair outside the solvent cage. So $\tau 1$ is our parameter of interest, and accounts to 1.20 ps.

The parameters obtained from this fitting procedure and those obtained for other alkylammonium nitrate ILs are similar [43], and endorse that the longer the alkyl chain the more long-lasting is the H-bond between cation and anion. To study the vibrational properties of the liquids, we cannot apply the standard Hessian diagonalization procedure, owing to the size of the system. This is way we decided to use a "dynamic approach" based on simulation trajectories. For each atom, the autocorrelation function of the velocity is calculated and the sum of all correlation functions of a molecule is Fourier transformed to get its power spectrum. Such power spectrum is finally projected onto the effective normal

Table 1
Normal modes of cation. The abbreviations in the text are: Tors. = torsion, Str. = stretching, Twist. = twisting, Rock. = Rocking, Wag. = wagging, Bend. = bending.

NM (cat.)	ω cm^{-1}	Type
1	444	H—C—N—H Tors.
2	978	C—N Str.
3, 4, 5, 6	958, 1238	Twist., Rock., Wag.
7	1414	H—C—N Bend.
8, 9	1458	H—C—N Bend.
10	1517	H—C—N Bend.
11, 12	1605	H—C—N Bend.
14	3050	C—H Str.
16	3146	C—H Str.
17	3155	C—H Str.

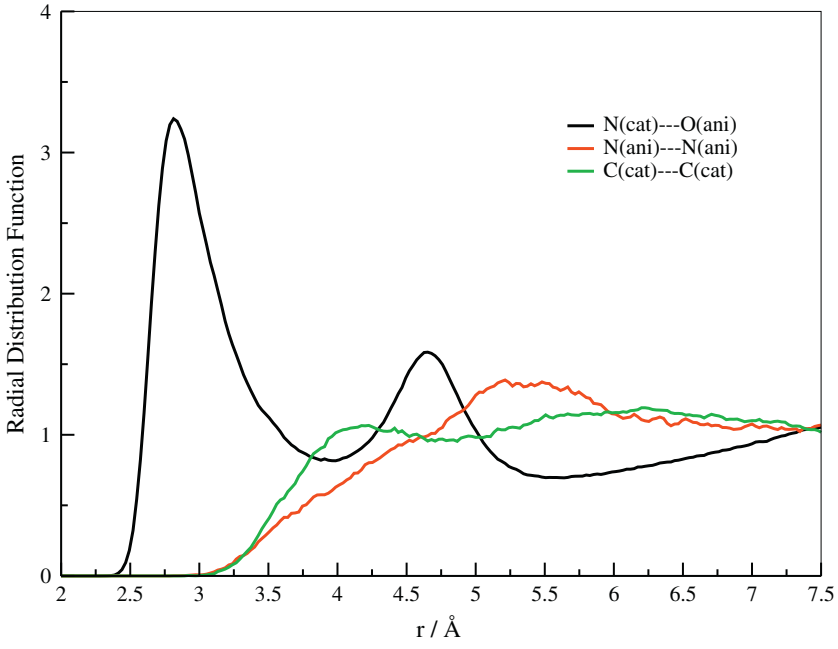

Fig. 4. Black line: RDFs between N···O distance. Green line: RDFs between nitrogen atoms of anions. Red line: RDFs between alyphatyc carbon atoms. (For interpretation of the references to color in this figure legend, the reader is referred to the web version of this article.)

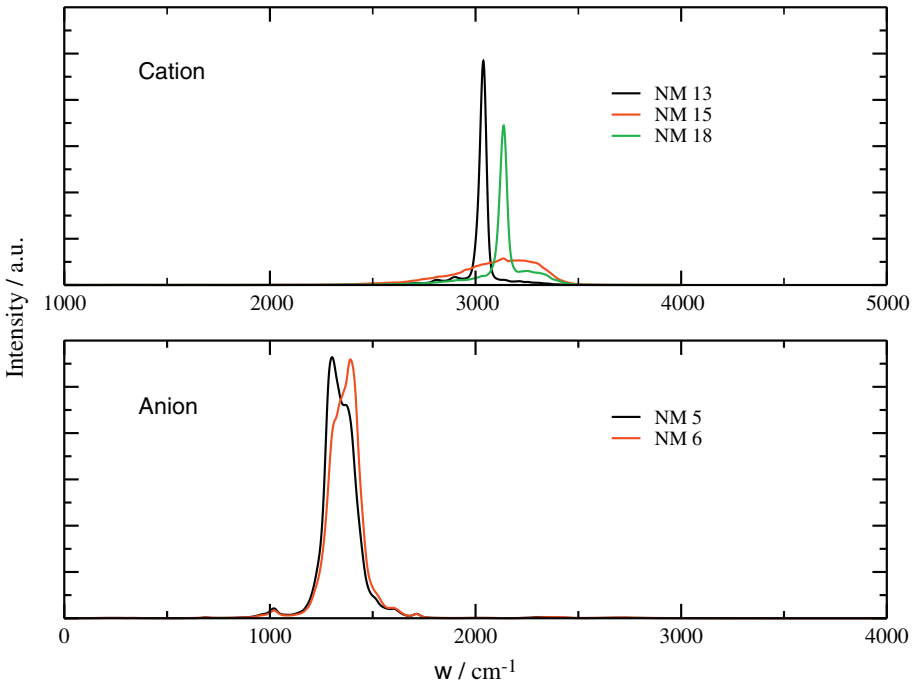

Fig. 5. Upper panel: N—H stretching normal modes VDOS for cation. Lower panel: VDOS of normal modes 5 and 6.

modes of the molecules to obtain the relative frequencies [30]. The effective normal modes (NM) for cation are reported in Table 1.

It can be seen how in the low frequency region ($\omega < 2000\ cm^{-1}$), the major contribution derives from the combination of bending and stretching of heavy/light atoms. In particular the normal modes from 3 to 6 results to be coupled and degenerate. The normal modes 13, 15 and 18, related to N—H stretching, are not reported in Table 1 because their relative VDOS are very broad, as it is shown in Fig. 5; this can be attributed to the polarization effect caused by H-bond network.

Finally the normal modes of anion are reported in Table 2.

The normal modes and frequencies were not compared with experimental results directly, since, unfortunately, no measurements could be performed on the system at such high temperature with our instrumentation. Though, it can be observed that they comply nicely with the data reported in a recent article by some of us on liquid 2-methoxyethylammonium nitrate ([30], Table II). In particular, we can notice that the in plane deformation normal modes are unaffected by hydrogen bond interaction and do not lose their degeneracy; on the contrary, the two antisymmetric stretching modes lose the degeneracy, but they are partially coupled (see their VDOS in Fig. 5). The frequency splitting between them is of about $90\ cm^{-1}$. This gap energy is in agreement with [30] and more recent studies [43].

Table 2
Normal modes of anion.

NM (ani.)	$\omega\ cm^{-1}$	Type
1, 2	698	In plane deformation
3	798	Out of plane
4	1027	Symmetric Str.
5, 6	1306, 1396	Asymmetric Str.

3. Conclusions

In this work, for the first time, the comparison between experimental X-ray scattering profile and classical-*ab initio* molecular dynamics simulations for melted methylammonium nitrate are reported. In our study we demonstrated how the classical molecular dynamics, without particular potential modification, fails in the reproduction of the experimental data, while the agreement between experiment and *ab initio* model is very good. Accordingly, the QM model allows to gather reliable and relevant structural information about the liquid phase. We find out a strong hydrogen bond network between cation and anion, with relative equilibrium distance between the hetero atoms (N(cat)···O(ani)) of 2.8 Å, in line with previous findings. In particular this is the only correlation distance present in this system, since the cation-cation and anion-anion RDF profile do not exhibit evident peaks. The lifetime of such contacts turns out to be 1.20 ps, and in a similar way to its upper analogues (EAN, PAN and BAN), not all the oxygen atoms of nitrate, but only two of them, are involved in durable hydrogen bonds. Finally, we have calculated the vibrational spectrum of both the cation and the anion using a dynamical approach, consisting in projecting the velocity density of states onto the effective normal modes of each molecule. Owing to the hydrogen bond network, the asymmetric normal modes of anion lose their degeneracy, and the resulting split is about $90\ cm^{-1}$. Instead, as far as the cation is concerned, we have shown how the cation-anion interaction leads to a broad velocity density of states for N—H stretching modes.

Acknowledgements

Financial support of the Scientific Committee of the University of Rome through Grants C26A13KR5Z, C26A142SCB and C26H13MNEB is gratefully acknowledged.

References

[1] P. Walden, Bull. Acad. Imper. Sci. (St. Petersburg) 8 (1914) 405–422.
[2] D.R. MacFarlane, K.R. Seddon, Aust. J. Chem. 60 (1) (2007) 3–5.
[3] E.W. Castner Jr., J.F. Wishart, J. Chem. Phys. 132 (12) (2010) 120901.
[4] G.J. Kabo, A.V. Blokhin, Y.U. Paulechka, A.G. Kabo, M.P. Shymanovich, J.W. Magee, J. Chem. Eng. Data 49 (3) (2004) 453–461.

[5] M. Petkovic, J.L. Ferguson, H.N. Gunaratne, R. Ferreira, M.C. Leitao, K.R. Seddon, L.P.N. Rebelo, C.S. Pereira, Green Chem. 12 (4) (2010) 643–649.
[6] G.-H. Tao, L. He, W.-S. Liu, L. Xu, W. Xiong, T. Wang, Y. Kou, Green Chem. 8 (7) (2006) 639–646.
[7] S. De Santis, G. Masci, F. Casciotta, R. Caminiti, E. Scarpellini, M. Campetella, L. Gontrani, Phys. Chem. Chem. Phys. 17 (32) (2015) 20687–20698.
[8] M. Campetella, E. Bodo, M. Montagna, S. De Santis, L. Gontrani, J. Chem. Phys. 144 (10) (2016).
[9] M. Campetella, S. De Santis, R. Caminiti, P. Ballirano, C. Sadun, L. Tanzi, L. Gontrani, RSC Adv. 5 (63) (2015) 50938–50941.
[10] M. Campetella, D. Martino, E. Scarpellini, L. Gontrani, Chem. Phys. Lett. 660 (2016) 99–101.
[11] R. Hayes, S. Imberti, G.G. Warr, R. Atkin, Angew. Chem. 52 (17) (2013) 4623–4627.
[12] P.A. Hunt, C.R. Ashworth, R.P. Matthews, Chem. Soc. Rev. 44 (5) (2015) 1257–1288.
[13] M. Campetella, L. Gontrani, F. Leonelli, L. Bencivenni, R. Caminiti, ChemPhysChem 16 (1) (2015) 197–203.
[14] A. Mariani, R. Caminiti, M. Campetella, L. Gontrani, Phys. Chem. Chem. Phys. 18 (4) (2016) 2297–2302.
[15] R.E. Wasylishen, Can. J. Chem. 64 (4) (1986) 773–776.
[16] H. Ishida, R. Ikeda, D. Nakamura, J. Chem. Soc., Faraday Trans. 2 (81) (1985) 963–973.
[17] M. Mylrajan, T.K.K. Srinivasan, G. Sreenivasamurthy, J. Crystallogr. Spectrosc. Res. 15 (5) (1985) 493–500.
[18] S. Zahn, J. Thar, B. Kirchner, J. Chem. Phys. 132 (12) (2010) 124506.
[19] E. Bodo, P. Postorino, S. Mangialardo, G. Piacente, F. Ramondo, F. Bosi, P. Ballirano, R. Caminiti, J. Phys. Chem. B 115 (45) (2011) 13149–13161.
[20] L. Tanzi, F. Ramondo, R. Caminiti, M. Campetella, A. Di Luca, L. Gontrani, J. Chem. Phys. 143 (11) (2015) 114506.
[21] M. Campetella, E. Bodo, R. Caminiti, A. Martino, F. D'Apuzzo, S. Lupi, L. Gontrani, J. Chem. Phys. 142 (23) (2015).
[22] G. Prampolini, M. Campetella, N. De Mitri, P.R. Livotto, I. Cacelli, J. Chem. Theory Comput. 12 (11) (2016) 5525–5540.
[23] L. Gontrani, E. Bodo, A. Triolo, F. Leonelli, P. DAngelo, V. Migliorati, R. Caminiti, J. Phys. Chem. B 116 (43) (2012) 13024–13032.
[24] X. Song, H. Hamano, B. Minofar, R. Kanzaki, K. Fujii, Y. Kameda, S. Kohara, M. Watanabe, S.-i. Ishiguro, Y. Umebayashi, J. Phys. Chem. B 116 (9) (2012) 2801–2813.
[25] R. Caminiti, V.R. Albertini, The kinetics of phase transitions observed by energy-dispersive x-ray diffraction, Int. Rev. Phys. Chem. 18 (2) (1999) 263–299.
[26] L. Gontrani, F. Ramondo, G. Caracciolo, R. Caminiti, J. Mol. Liq. 139 (1–3) (2008) 23–28.
[27] L. Gontrani, F. Ramondo, R. Caminiti, Chem. Phys. Lett. 417 (1) (2006) 200–205.
[28] M. Campetella, L. Gontrani, E. Bodo, F. Ceccacci, F.C. Marincola, R. Caminiti, J. Chem. Phys. 138 (18) (2013) 184506.
[29] M. Usula, F. Mocci, F.C. Marincola, S. Porcedda, L. Gontrani, R. Caminiti, J. Chem. Phys. 140 (12) (2014) 124503.
[30] M. Campetella, D. Bovi, R. Caminiti, L. Guidoni, L. Bencivenni, L. Gontrani, J. Chem. Phys. 145 (2) (2016) 024507.
[31] J. Wang, R.M. Wolf, J.W. Caldwell, P.A. Kollman, D.A. Case, J. Comput. Chem. 25 (9) (2004) 1157–1174.
[32] L. Martínez, R. Andrade, E.G. Birgin, J.M. Martínez, J. Comput. Chem. 30 (13) (2009) 2157–2164.
[33] J. Hutter, M. Iannuzzi, F. Schiffmann, J. VandeVondele, Wiley Interdiscip. Rev. Comput. Mol. Sci 4 (1) (2014) 15–25.
[34] J. VandeVondele, J. Hutter, J. Chem. Phys. 118 (10) (2003) 4365–4369.
[35] S. Grimme, J. Comput. Chem. 27 (15) (2006) 1787–1799.
[36] C. Hartwigsen, S. Gœdecker, J. Hutter, Phys. Rev. B 58 (7) (1998) 3641.
[37] D. Bovi, A. Mezzetti, R. Vuilleumier, M.-P. Gaigeot, B. Chazallon, R. Spezia, L. Guidoni, Phys. Chem. Chem. Phys. 13 (47) (2011) 20954–20964.
[38] P.H. Hünenberger, J.A. McCammon, J. Chem. Phys. 110 (4) (1999) 1856–1872.
[39] J.C. Araque, J.J. Hettige, C.J. Margulis, J. Phys. Chem. B 119 (40) (2015) 12727–12740.
[40] E. Bodo, A. Sferrazza, R. Caminiti, S. Mangialardo, P. Postorino, J. Chem. Phys. 139 (14) (2013) 144309.
[41] W. Humphrey, A. Dalke, K. Schulten, J. Mol. Graph. 14 (1) (1996) 33–38.
[42] M. Brehm, B. Kirchner, J. Chem. Inf. Model. 51 (8) (2011) 2007–2023.
[43] M. Campetella, M. Macchiagodena, L. Gontrani, B. Kirchner, Mol. Phys. 115 (13) (2017) 1582–1589.